

4-Phenylcoumarins from *Mesua ferrea* with selective CYP1B1 inhibitory activity

Fengxu Zhou

Kunming Medical University

Ruoyue Huang

Sichuan University West China Hospital

Tingting Cao

Kunming Medical University

Jia Liu

Kunming Medical University

Weimin Yang

Kunming Medical University

Fei Li

Sichuan University West China Hospital

Xian Li (✉ xianlikm@163.com)

Kunming Medical University

Research Article

Keywords: Clusiaceae, *Mesua ferrea* Linn, 4-phenylcoumarin, CYP1B1 inhibitory activity

Posted Date: May 12th, 2022

DOI: <https://doi.org/10.21203/rs.3.rs-1610077/v1>

License:   This work is licensed under a Creative Commons Attribution 4.0 International License.

[Read Full License](#)

Abstract

Three new 4-phenylcoumarins, mesuaferlinns A–C (1–3), together with ten known 4-phenylcoumarins, 4–13, were isolated from the branches and leaves of *Mesua ferrea* Linn. (Clusiaceae). The structure of compounds 1–3 were determined on the basis of spectroscopic methods including extensive analysis of NMR and mass spectroscopic data. Ten 4-phenylcoumarins were tested for their cytochrome P450 family 1 enzymes (CYP 1A1, CYP 1A2, and CYP 1B1) inhibitory effects. Compounds 5 and 10 were found to be the most potent two CYP1B1 inhibitors with inhibitory viabilities values of 56.64% and 47.46%.

Introduction

P450 family 1 enzymes include CYP 1A1, CYP 1A2, and CYP 1B1, which are important environmental xenobiotic-metabolizing enzymes. Cytochrome P450 1B1 (CYP 1B1) is a heme-thiolate monooxygenase involved in NADPH-dependent phase I metabolism of a variety of xenobiotics such as ethoxyresorufin, theophylline and caffeine, and shows activity toward activation of environmental carcinogens via the hydroxylation of procacinoxens, including 27 polycyclic aromatic hydrocarbons and their derivatives, 17 heterocyclic and aryl amine and aminoazo dyes, 3 mycotoxins, 2 nitroaromatic hydrocarbons [1–2]. Different from P450s 1A1 and 1A2, CYP 1B1 expression is not detected in human liver, but CYP 1B1 is expressed in many extrahepatic tissues, including lung, colon, eye, kidney and also highly expressed in a wide of variety of cancers, such as prostate, uterus, and colon cancer. Therefore, selective inhibition of P450 1B1 is a potential molecular target for chemoprevention of environmental hydroxylation-caused DNA mutations and carcinogenesis. Coumarin is a kind of important compounds which have been shown to effectively inhibit CYP 1B1, but coumarin has its potential ability to activate the aryl hydrocarbon receptor (AhR), which may lead to up-regulation of P450 [3–4]. In this work, to obtained new and selective P450 1B1 inhibitors, we performed a two-step design, isolation and evaluation on P450 family 1 enzymes.

The species *Mesua ferrea* Linn. belongs to the family Clusiaceae, which is a medium-to-large sized evergreen tree. Generally, it is widely distributed in Southeast Asia, India, and Sri Lanka. The dried floral bud of this plant is commonly known in India as Nagakesara and traditionally used as brain tonic appetizer, antiemetic, anthelmintic, aphrodisiac diuretic and antidote [5–6]. Previous studies on *M. ferrea* resulted in the isolation of xanthenes, coumarins, triterpenoids, biflavones, cyclohexanedione derivatives, and an essential oil. Most of these isolated compounds were reported to show cytotoxic and antibacterial activities [7–12]. In our ongoing search for selective and inhibitory P450 1B1 coumarins from this plant, an investigation of the chemical constituents of *Mesua ferrea* Linn., which was collected in Gengma county, Yunnan Province, led to isolation of three new 4-phenylcoumarins, mesuaferlinns A–C (1–3), together with ten known 4-phenylcoumarins, 4–13. This report deals with the isolation and characterization of the new 4-phenylcoumarins. In addition, we describe the inhibitory effects of these 4-phenylcoumarins isolated in this study on P450 family 1 enzymes. And to identify the influence of tested inhibitors on CYP1B1 expression, an AhR-signaling assay was also performed.

Results And Discussion

Structure Elucidation

Mesuaferlinn A (**1**) (Fig. 1) was obtained as a yellow gum, and its positive HR-ESI-MS spectrum showed $[M + Na]^+$ at m/z 443.1467, consistent with the molecular formula $C_{25}H_{24}O_6$. The UV spectrum suggested a 5,7-dioxygenated coumarin, with absorptions at λ_{max} 237, 290, and 363 nm [13]. The IR spectrum of **1** showed bands indicating the presence of hydroxyl groups (ν_{max} 3434 cm^{-1}), an α , β -unsaturated lactone (ν_{max} 1721 cm^{-1}) and a chelated acyl group (ν_{max} 1612 cm^{-1}) [14].

The characteristic singlet of H-3 of a 4-substituted coumarin was observed at $\delta(H)$ 6.07 ppm. And the presence of a monosubstituted phenyl group at C-4 was deduced by the presence of five aromatic proton signal at $\delta(H)$ 7.42 (5H, m), in combined with key HMBC correlations (Fig. 2) from H-3 to the quaternary aromatic carbon C-1' ($\delta(C)$ 140.26) and IR spectrum with absorptions at 767 cm^{-1} and 703 cm^{-1} . Furthermore, the 1H NMR spectrum of **1** also showed a phenolic hydroxyl signal at $\delta(H)$ 14.72, exchangeable with D_2O , and probably strongly chelated by the carbonyl function of an acyl group. These observations supported the presence of an 8-acyl-5,7-dioxygenated-4-phenyl-coumarin type.

The 1H NMR spectrum showed an olefinic singlet at δ 6.98 (1H, s, H-3''), and two methyl groups as a six-proton singlet at δ 1.71 (3H, s, H-5'') and 1.71 (3H, s, H-6''). In the HMBC spectrum, the correlations were observed for the H-3'' with C-6 ($\delta(C)$ 111.29), C-5 ($\delta(C)$ 154.38), C-7 ($\delta(C)$ 165.19), the two methyl groups of H-5'' and H-6'' with the oxygenated quaternary carbon C-4'' ($\delta(C)$ 68.9) and olefinic carbon C-2'' ($\delta(C)$ 163.8), attributed to the presence of a furan moiety. The 1H NMR spectrum exhibited two methyls resonating as a doublet and a triplet respectively, which indicated the presence of a 2-methylbutyl moiety in **1**. And on the basis of the COSY experiment, the cross correlations of H-2''' ($\delta(H)$, 3.96) with H-5''' ($\delta(H)$, 1.26), H-3'''a ($\delta(H)$, 1.93), H-3'''b ($\delta(H)$, 1.52) and H-3'''a, H-3'''b with H-4''' ($\delta(H)$, 0.99) which combined the HMBC correlations H-2''' and H-3''' correlated with a carbonyl (C-1'''), identified the presence of 2-methylbutanoyl substituent, as shown in Fig. 2. In the HMBC spectrum, C-OH ($\delta(H)$ 14.72) correlated with a carbonyl (C-1'''), together with the 1H , ^{13}C NMR, UV, and IR spectra (Table 1) which indicated the presence of a coumarin skeleton with all positions substituted except C-3 and 8-acyl-5,7-dioxygenated-coumarin type, hence confirming the attachment of the 2-methylbutanoyl group at position C-8 in the coumarin skeleton. Assignments of the 1H and ^{13}C NMR resonances of compound **1** (Table 1), which was named mesuaferlinn A, were determined through analysis of its COSY, HMQC, and HMBC data.

Table 1
¹H- and ¹³C-NMR spectral data for compounds **1-3** (in Acetone-d₆).

position	1		2		3	
	δ(C)	δ(H)	δ(C)	δ(H)	δ(C)	δ(H)
2	159.2		159.2		159.7	
3	114.9	6.07 (s)	114.8	6.07 (s)	112.3	5.83 (s)
4	157.3		157.3		157.4	
5	156.2		156.1		164.2	
6	111.4		111.3		107.6	
7	165.3		165.3		164.6	
8	105.4		105.4		106.4	
9	154.5		154.4		159.0	
10	103.9		103.4		102.3	
1'	140.4		140.4		140.9	
2',6'	128.2	7.42 (<i>m</i> , overlapped)	128.2	7.43 (<i>m</i> , overlapped)	128.1	7.35 (<i>m</i>)
3',5'	128.5	7.42 (<i>m</i> , overlapped)	128.5	7.43 (<i>m</i> , overlapped)	128.5	7.39 (<i>m</i> , overlapped)
4'	129.1	7.42 (<i>m</i> , overlapped)	129.0	7.43 (<i>m</i> , overlapped)	128.8	7.39 (<i>m</i> , overlapped)
1''					213.3	
2''	163.8		163.7		40.5	4.09 (<i>m</i>)
3''	98.4	6.98 (s)	98.3	6.98 (s)	19.6	1.14 (<i>d</i> , <i>J</i> = 6.7)
4''	68.9	4.67 (s, -OH)	68.9	4.67 (s, -OH)	19.6	1.14 (<i>d</i> , <i>J</i> = 6.7)
5''	29.3	1.71 (s)	29.2	1.70 (s, overlapped)		
6''	29.3	1.71 (s)	29.2	1.70 (s, overlapped)		
1'''	209.8		209.9			
2'''	46.7	3.96 (<i>m</i>)	40.2	4.07 (<i>m</i>)	77.4	4.54 (brd, <i>J</i> = 7.6)
3'''a	27.2	1.93 (<i>m</i>)	19.1	1.28 (<i>d</i> , <i>J</i> = 6.8)	30.7	3.07 (<i>dd</i> , <i>J</i> = 15.0, 8.0)

position	1		2		3	
	$\delta(\text{C})$	$\delta(\text{H})$	$\delta(\text{C})$	$\delta(\text{H})$	$\delta(\text{C})$	$\delta(\text{H})$
3 ^{'''} b		1.52 (<i>m</i>)				3.26 (<i>dd</i> , <i>J</i> = 15.0, 2.2)
4 ^{'''}	12.1	0.99 (<i>t</i> , <i>J</i> = 7.4)	19.1	1.28 (<i>d</i> , <i>J</i> = 6.8)	147.4	
5 ^{'''} a	16.5	1.26 (<i>d</i> , <i>J</i> = 6.7)			111.0	4.87 (<i>s</i>)
5 ^{'''} b						5.06 (<i>s</i>)
6 ^{'''}					18.8	1.90 (<i>s</i>)
δ in ppm, <i>J</i> in Hz. ¹ H-NMR: 600 MHz, ¹³ C-NMR: 150 MHz.						

Mesuaferlinn B (**2**) was isolated as a yellow gum. The HR-ESI-MS spectrum revealed a pseudomolecular ion peak $[\text{M} + \text{Na}]^+$ at m/z 429.1307, which corresponded to the molecular formula $\text{C}_{24}\text{H}_{22}\text{O}_6$. The UV spectrum supported 5,7-dioxy-coumarin type, with absorptions at λ_{max} 232, 289, and 360 nm [13]. The IR spectrum exhibited strong absorptions at ν_{max} 1371 cm^{-1} due to a gem-dimethyl, a peak at 1611 cm^{-1} belonging to a chelated acyl group and a broad peak at 3434 cm^{-1} due to a chelated hydroxyl group stretching [14].

All protons and carbons were assigned by analysis of 1D and 2D NMR spectroscopic data. The NMR spectroscopic data of **2** was quite close to those of **1**, except that an iso-propyl group attached to carbonyl C-1^{'''} ($\delta(\text{C})$ 209.9) in place of a 2-methylbutanoyl moiety in **1**. The key ¹H-¹H COSY correlations (Fig. 2) of a multiplet at $\delta(\text{H})$ 4.07 (H-2^{'''}) with a doublet at $\delta(\text{H})$ 1.28 (*d*, H-3^{'''} and H-4^{'''}), in combined with key HMBC correlations (Fig. 2) from H-2^{'''}, H-3^{'''} and H-4^{'''} to C-1^{'''}, confirmed that an iso-propyl group attached to carbonyl C-1^{'''}. Therefore, extensive spectroscopic analysis by using COSY, HSQC and HMBC NMR spectra confirmed the structure of **2** as mesuaferlinn B.

Mesuaferlinn C (**3**) was obtained as a yellow gum, and its molecular formula $\text{C}_{24}\text{H}_{22}\text{O}_5$ was established by positive HR-ESI-MS analysis of its protonated molecule $[\text{M} + \text{H}]^+$ at m/z 391.1541. The UV spectrum supported a 5,7-dihydroxy-coumarin type, with absorptions at λ_{max} 229, 283 and 372 nm. The IR spectrum showed absorptions at ν_{max} 3430 (chelated OH), 1620 (chelated acyl group) and 1383 cm^{-1} (gem-dimethyl). The ¹H NMR spectrum of **3** (Table 1) showed the presence of a singlet at $\delta(\text{H})$ 5.83 characteristic for H-3 of a 4-substituted coumarin, a 2-methylbutanoyl moiety [$\delta(\text{H})$ 4.09 (1H, *m*, H-2^{'''}), 1.14 (3H, *d*, *J* = 6.7, H-3^{'''}), 1.14 (3H, *d*, *J* = 6.7, H-4^{'''}) and $\delta(\text{C})$ 213.3 (C-1^{'''}), 40.5 (C-2^{'''}), 19.6 (C-3^{'''}), 19.6 (C-4^{'''})], a 2-(1-methylethenyl)-dihydrofuran moiety [$\delta(\text{H})$ 4.54 (1H, *brd*, H-2^{'''}), 3.26 (1H, *dd*, H-3^{'''}b), 3.07 (1H, *dd*, H-3^{'''}a), 5.06 (1H, *s*, H-5^{'''}b), 4.87 (1H, *s*, H-5^{'''}a), 1.90 (3H, *s*, H-6^{'''}) and $\delta(\text{C})$ 77.4 (C-2^{'''}), 30.7 (C-3^{'''}), 147.4 (C-4^{'''}), 111.0 (C-5^{'''}), 18.8 (C-6^{'''})]. The key ¹H-¹H COSY correlations (Fig. 2) of H-2^{'''} with H-3^{'''} and H-4^{'''}, in

combined with key HMBC correlations (Fig. 2) from H-2", H-3" and H-4" to C-1", confirmed that an isopropyl group attached to carbonyl C-1". Together with the ¹H and ¹³C NMR spectra (Table 1) which indicated the presence of a coumarin skeleton with all positions substituted except C-3, hence confirming the attachment of the oxo-butyryl group at position C-6 in the coumarin skeleton. In addition, the HMBC correlations clearly proved that the substituted dihydrofuran ring is located between δ(C)C-7 (s, 164.6) and C-8 (s, 106.4) by exhibiting the following correlations H-3"^{a, b}/C-7, C-8, and H-2"/ C-8. A close comparison of the NMR data of **3** with those of the known compound mammea A/AA deshydrocyclo F indicated that the two compounds were identical except for the acyl substituents at C-6[13]. Considering the structural resemblances of compound **3** and mammea A/AA deshydrocyclo F, the relative configuration of C-2 of **3** was suggested to be β due to the key REOSY correlations of H-2" (δ(H) 4.54) with H-3"^a (δ(H) 3.07) and H-3"^b (δ(H) 3.26), in combined with lacking direct ROESY correlations of H-5"^a (δ(H) 4.87), H-5"^b (δ(H) 5.06) and H-6" (δ(H) 1.90) with H-3"^a and H-3"^b (Fig. 2). So, the complete structural elucidation of **3** as mesuaferlin C was made with the aid of COSY, HMQC, HMBC and ROESY spectra.

The structures of the ten known coumarins were identified as 8,9-dihydro-5-hydroxy-6-(2-methylbutanoyl)-4-phen-yl-8-(prop-1-en-2-yl)furo[2,3-h]chrome-2-one (**4**)[7], mammea A/BD(**5**)[16], mammea A/BB (**6**)[16], mammea A/AD cyclo D(**7**)[7], mammea A/AB cyclo D(**8**)[7], mammea A/AB cyclo E(**9**)[17], mammea A/AB cyclo F(**10**)[7], mammea A/AD cyclo F (**11**)[7], mammea A/AB (**12**)[7], mammea A/BB cyclo F (**13**)[13], by comparison of their spectral data with values reported in the literature.

Inhibitory Activities of Isolated 4-Phenylcoumarins toward P450s 1A1, 1A2, and 1B1

Ten 4-Phenylcoumarins isolated from *M. ferrea* Linn. were tested in incubated on microsomes in vitro in order to determine their inhibitory activities and selectivity toward P450 1B1 (Table 2). The most potent compounds (**5** and **10**) toward P450 1B1 possesses inhibitory viabilities values of 56.64% and 47.46%, respectively. In addition, the data show that furanocoumarin derivatives are more potent than the other coumarin derivatives in inhibiting P450 1B1.

Table 2
Inhibitory activities of tested compounds on CYP1 enzymes

Compd.	Inhibition ratio (%)		
	CYP1A1	CYP1A2	CYP1B1
1	26.31	6.79	42.94
2	18.63	16.31	5.76
4	0.83	8.45	14.62
5	23.75	8.23	56.64
6	29.90	2.75	20.92
7	19.76	6.85	-13.00
8	30.96	8.71	41.92
9	18.04	1.38	12.17
10	20.45	1.98	47.46
11	25.97	-0.10	-17.10
Positive*	14.85	50.13	43.84

*: Using α -naphthalenone as positive control of CYP1A1 and CYP1A2; Using resveratrol as positive control of CYP1B1.

Effects on Activation of AhR

The aryl hydrocarbon receptor (AhR) is a ligand-activated transcriptional factor that dimerizes with aryl hydrocarbon receptor nuclear translocator (ARNT) [18]. And it was reported that CYP 1A1 performs as target gene of AhR [19]. To determine whether the expression of AhR is functionally relevant, six compounds were given further QPCR experiment. And the results of the QPCR experiment suppose that at the gene level, all compounds can significantly activate the AhR target gene CYP1A1(Fig. 3).

Evaluation of nicotinamide adenine dinucleotide phosphate (NADPH) Dependent Experiment

In order to further demonstrate the formation of inhibitory activity of tested compound, the reactive metabolites 4-Hydroxy- β -estradiol produced in mouse liver microsomes (MLMs) was determined. Respectively, estradiol was transformed to 4-Hydroxy- β -estradiol in the NADPH-regenerating system, whereas the conjugates could not be detected in the MLMs incubation without NADPH (Fig. 4).

Conclusions

The 13 coumarins isolated from *M. ferrea* Linn., including three new coumarins, shows similarities of a phenyl group in C-4, an isopentenyl or acyl group in C-6 or C-8. Generally, these coumarins can be classified into three groups: simple coumarin, pyranocoumarin, and furanocoumarin. And ten of them was tested with mouse liver microsomes culture experiment of CYP1 enzymes, and exhibited varied levels of inhibitory potencies. Almost compounds display inhibitor activities to CYP1A1 except compound **4**, which is totally different from the opposite of non inhibitor to CYP1A2. Compounds **5** and **10** were found to be the most potent two CYP1B1 inhibitors with inhibitory viabilities values of 56.64% and 47.46%. and as a general trend, furanocoumarin was more active than other coumarins in CYP1B1 inhibition. Further AhR signaling experiment has taken in 6 compounds, and all of them can activate the AHR target gene CYP1A1. NADPH dependent experiment indicate that the compounds can take CYP1B1 inhibitory activity in NADPH involved situation.

Experimental Section

General

Optical rotations were recorded on a JASCO P-1020 automatic digital polarimeter. UV spectra were measured on a Shimadzu UV-2401 PC ultraviolet spectrometer, and IR data were carried out on a BRUKER Tensor-27 Fourier transform infrared spectrometer, respectively. NMR spectra were obtained on a Bruker Avance III 600 MHz spectrometer. The chemical shifts are given in ppm with TMS (tetramethylsilane) as an internal reference, and coupling constants are reported in Hz. ESI-MS and HRESI-MS data were recorded on an Agilent G6230 time-of-flight mass spectrometer. Semipreparative HPLC was run on a LC-5510 analytical and semi-preparative high-performance liquid chromatographs with a Zorbax SB-C18 column (Agilent, 4.6 mm×250 mL, 5 μm). And preparative HPLC was run on a Waters 1525 High Performance Liquid Chromatograph with a Waters SunFire C18 column. TLC was run on precoated silica gel plates, using 10% ethanol-H₂SO₄ as a visualization reagent. ODS RP-18 (40–60 μm, Merck, Germany), Sephadex LH-20 (GE Healthcare Bio-Sciences Corp, Piscataway, USA), macroporous resin (D101 type, Mitsubishi Corporation, Japan), and silica gel (200 – 300 mesh, Qingdao Haiyang Chemical Co., Ltd., People's Republic of China) were used for column chromatography.

Reagents.

Nicotinamide adenine dinucleotide phosphate (NADPH) were obtained from Sigma-Aldrich (St. Louis, MO, USA). Mouse liver microsomes (MLMs) were obtained from Research Institute for Liver Diseases (Shanghai) Co., Ltd. The inhibitor resveratrol and 6-Naphthoflavone were purchased from Shanghai Maclin Biochemical Technology Co., LTD or Shanghai yuanye Bio-Technology Co., Ltd. β-estradiol were also purchased from Shanghai Maclin Biochemical Technology Co., LTD. 4-hydroxyestradiol were purchased from Cayman Chemical Company. All solvents (methanol and acetonitrile) were UPLC-MS (ultraperformance liquid chromatography-mass spectrometry) grade and reagents were analytical grade.

Plant material

The branches and leaves of *M. ferrea* were collected in Gengma, Yunnan Province, People's Republic of China, in April 2018, and identified by Prof. Li-ping Tang of Kunming Medical University. And the voucher specimen (No. 20180430) was deposited at Kunming Medical University.

Extraction and isolation

The air-dried branches and leaves of *M. ferrea* (5 kg) were extracted exhaustively with 95% EtOH-H₂O (24 h × 3) at room temperature, followed by filtration. The filtrates were combined and evaporated under reduced pressure to afford an extract (500 g). The dried extract was subjected to silicagel column chromatography and sequentially partitioned by eluting with petroleum ether, chloroform, EtOAc, acetone, and MeOH to afford five fractions (A-E).

Fraction B (61 g) was then separated by column chromatography over silica gel (200 – 300 mesh) with a gradient mixture of petroleum ethyl-EtOAc (200:1→0:1, v/v) to yield 20 fractions (Fr. 1–20). Then, Fr. 9 was applied to a silica gel column (200 – 300 mesh) and eluted with a gradient mixture of petroleum ethyl-EtOAc (80:1→1:1, v/v) and further purified by semi-preparative HPLC with acetonitrile-H₂O-Acetic acid (85:15:0.5, v/v) to yield compound **8**. Fr. 10 was chromatographed on a silica gel column with petroleum ethyl-chloroform (10:1→1:1, v/v) and then purified by semi-preparative HPLC, run isocratically using a mixture of MeOH-H₂O (84:16, v/v), affording compound **13**. Fr. 11 was subjected to passage over a Sephadex LH-20 column by elution with acetone to yield four subfractions (Fr. 11 – 1 – 11 – 4). The main fraction, Fr. 11 – 3 was then separated chromatographically on a preparative HPLC column with MeOH-H₂O (90:10, v/v) to yield Fr. 11-3-1 – 11-3-4. Fr.11-3-1 was purified by semi-preparative HPLC with MeOH-H₂O (90:10, v/v) to produce compound **5**. Fr.11-3-2 was subjected to separation using semi-preparative HPLC with acetonitrile-H₂O-Acetic acid (90:10:0.5, v/v), affording compound **7**. Fr. 11-3-3 was separated chromatographically by semi-preparative HPLC column with acetonitrile-H₂O-Acetic acid (87:13:0.5, v/v) to yield compound **6**. And Fr. 11-3-4 was purified by semi-preparative HPLC with acetonitrile-H₂O-Acetic acid (85:15:0.5, v/v), affording compound **1**. Fr. 12 was fractionated over Sephadex LH-20 using acetone to furnish eleven fractions (Fr. 12 – 1 – 12 – 11). The main part Fr. 12 – 9 was submitted to silicagel column chromatography and eluted with a gradient of petroleum ethyl-acetone (70:1→1:1, v/v) to afford ten fractions (Fr. 12-9-1 – 12-9-10). Fr. 12-9-6 was purified by semi-preparative HPLC with MeOH-H₂O (85:15, v/v) to get compounds **10** and **12**. Fr. 12-9-10 on preparative TLC over silica gel using petroleum ethyl-EtOAc (3:1, v/v) yielded compound **9**. Fr. 13 was subjected to separation over a Sephadex LH-20 column with acetone as the eluent, to yield thirteen subfractions (Fr. 13 – 1 – 13–13). Fr. 13 – 6 was applied to a silica gel column and eluted with a gradient mixture of petroleum ethyl-acetone (100:1→1:1, v/v) to yield thirteen subfractions (Fr. 13-6-1 – 13-6-13). Fr. 13-6-11 was subjected to separation using semi-preparative HPLC with acetonitrile-H₂O-Acetic acid (85:15:0.5, v/v), affording compounds **3** and **4**. Fr. 13-6-13 was purified by semi-preparative HPLC with MeOH-H₂O (85:15, v/v) to produce compounds **2** and **11**.

Mesuaferlin A (**1**). Yellow gum. $[\alpha]_D^{21} = +4.95$ ($c = 0.124$, MeOH). UV(MeOH) λ_{max} (log ϵ): 363(3.73), 290(4.38), 237(4.29), 206(4.51) nm; IR(KBr): 3434, 3059, 3030, 2974, 2934, 2876, 1749, 1721, 1612, 1476,

1372, 1177, 1145, 945, 859, 767, 703 cm^{-1} . ESI-MS: 443 $[\text{M} + \text{Na}]^+$; HR-ESI-MS: 443.1467 ($[\text{M} + \text{Na}]^+$, $\text{C}_{25}\text{H}_{24}\text{O}_6\text{Na}$; calc.443.1471). ^1H - and ^{13}C -NMR: see Table 1.

Mesuaferlinn B (**2**). Yellow gum. $[\alpha]_D^{21} = +6.91$ ($c = 0.118$, MeOH); UV(MeOH) λ_{max} ($\log \epsilon$): 360(3.72), 289(4.36), 232(4.28), 204(4.52) nm; IR (KBr): 3434, 3059, 3029, 2978, 2934, 2874, 1749, 1722, 1611, 1476, 1371, 1181, 1146, 951, 858, 766, 703 cm^{-1} . ESI-MS: 429 $[\text{M} + \text{Na}]^+$; HR-ESI-MS: 429.1307 ($[\text{M} + \text{Na}]^+$, $\text{C}_{24}\text{H}_{22}\text{O}_6\text{Na}$; calc.429.1314). ^1H - and ^{13}C -NMR: see Table 1.

Mesuaferlinn C (**3**). Yellow gum. $[\alpha]_D^{22} = +6.55$ ($c = 0.127$, MeOH). UV(MeOH) λ_{max} ($\log \epsilon$): 405(3.77), 372(3.83), 283(4.22), 229(4.16), 204(4.46) nm; IR (KBr): 3430, 3059, 3030, 2969, 2931, 2873, 1712. 1620, 1585, 1428, 1379, 1130, 906, 853, 768, 700 cm^{-1} . ESI-MS: 391 $[\text{M} + \text{H}]^+$; HR-ESI-MS: 391.1541 ($[\text{M} + \text{H}]^+$, $\text{C}_{24}\text{H}_{23}\text{O}_5$; calc.391.1546). ^1H - and ^{13}C -NMR: see Table 1.

Enzyme Activity Inhibition Assays of CYP1A1, CYP1A2 and CYP1B1

The methods for measuring CYP enzyme activity were described in previous literature [20] and were briefly described as follows: the incubation system was carried out in 96-well plates, and the reaction system consists of β -estradiol (20 μM), the chemical inhibitor or the compound, which the concentration was the same as that of the inhibitor, MLM (0.5mg/ml), and buffer solution (PBS, PH = 7.4). The chemical inhibitors of CYP1A1, CYP1A2 and CYP1B1 enzyme activity were α -naphthalenone (10.0 μM), α -naphthalenone (1.0 μM) and resveratrol (10 μM), respectively. After the reaction system was incubated, NADPH was added for reaction, the reaction was terminated and centrifuged, and the supernatant was taken for testing to determine the inhibitory effect of the compounds on CYP1s activity by UPLC-MS. Incubation system in triplicate. The groups were as follows: ☐Positive group: the inhibitory, β -estradiol and NADPH. ☐Negative group: no NADPH, replaced with equal volume PBS. ☐Experimental group: β -estradiol, the compound and NADPH.

A series of compounds were added to the incubation system to test IC_{50} , which was the same as that of CYPs inhibition assay (the final concentration in the system was 1, 5, 20, 50, 100 μM).

UPLC-ESI-QTOF-MS Analysis

All samples were analyzed on a high-resolution Q Exactive Plus hybrid quadrupole-Orbitrap Mass Spectrometer (Thermo Fisher Scientific, San Jose, CA). The drug metabolites were transported on an XDB-C18 column (2.1 \times 100 mm, 1.8mm, Agilent, Santa Clara, CA). The injection volume was 5 μl , and the liquid flow was 0.3 ml/min. Phase A was 0.01% formic acid aqueous solution, and phase B was acetonitrile containing 0.01% formic acid. The elution gradient was as follows: 0–12 min, 2–98%B; 12–14 min, 98%B; 14–16 min, 98%A. The column temperature was 45 $^\circ\text{C}$. The data were in positive ion mode. The flow rate of collision gas and dry gas was 9 L/min. Capillary voltage 3.5 kV, temperature 350 $^\circ\text{C}$, atomizer pressure 35 psi.

NADPH-Dependency Assay

The incubation system and the samples analysis of the assay was the same as that of CYPs inhibition assay. The groups were as follows: Sample group: β -estradiol, the compound and NADPH. N-NADPH group: β -estradiol and the compound, no NADPH, with equal volume of PBS instead. Control group: β -estradiol and NADPH.

Cell Culture and Cell Activity Assay

The human hepatoma cell line HepG2 were purchased from Culture Collection of the Chinese Academy of Sciences (Shanghai, China) and tested by STR. The cells were preserved in Dulbecco's modified Eagle medium (DMEM), supplemented with 1% penicillin-streptomycin solution and 10% fetal bovine serum in a humidified environment of 37°C and 5% CO₂. 2×10⁴ cells/well were cultured on 96-well plates in 200 μ L DMEM medium, and the cells were incubated with compounds (2.5, 12.5, 25 or 100 μ M) for 24h, then MTT solution was added to detect the cell activity.

AhR-Signaling Assay

Compounds or diosmine, the AHR agonist, were added to cells to determine the effect of compounds on AHR signaling pathways. 2×10⁴ cells/well were cultured on 12-well plates in 2 mL DMEM medium, and the cells were incubated with compounds (25 μ M) or diosmin (25 μ M) for 24h. RNA for the cells was extracted and QPCR was performed to determine the expressions of CYP1A1 mRNA.

Data and statistical analysis

Chromatographic and spectral data were analyzed using QE Plus data acquisition software. All values were expressed as mean \pm SD, and Graphpad Prism software 9.0 (Inc., La Jolla, CA)) was used for statistical analysis to obtain IC₅₀ value.

Declarations

Data Availability Statements

The data that supports the findings of this study are available in the supplementary information of this article.

Acknowledgements

The authors are grateful to acknowledge the financial support from the Yunnan Provincial Science and Technology Department (NoS.2019HB025, 202005AE160004, 202005AF150043) and the National Natural Science Foundation of China (31860087).

Author Contribution Statement

Feng-Xu Zhou performed the experiments, including isolation, structure identification, and prepared the manuscript. Ruo-Yue Huang has contributed to the study of active compounds and the writing of active parts. Ting-Ting Cao and Jia Liu performed the auxiliary experiments. Dr. Wei-Min Yang guided the experiments. Dr. Fei Li and Dr. Xian Li were the supervisor of the present work, checked the structure determination of the isolated compounds and the biological study, and completed the redaction of the article. All authors revised and approved the final version of the manuscript.

References

1. Pottenger LH, Christou M, Jefcoate CR (1991) Purification and immunological characterization of a novel cytochrome P450 from C3H/10T1/2 cells. Arch Biochem Biophys 286(2):488–497. [https://doi.org/10.1016/0003-9861\(91\)90070-Y](https://doi.org/10.1016/0003-9861(91)90070-Y)
2. Savas U, Bhattacharyya KK, Christou M, Alexander DL, Jefcoate CR (1994) Mouse cytochrome P-450EF, representative of a new 1B subfamily of cytochrome P-450s. Cloning, sequence determination, and tissue expression. J Biol Chem 269(21):14905–14911. [https://doi.org/10.1016/S0021-9258\(17\)36551-1](https://doi.org/10.1016/S0021-9258(17)36551-1)
3. Li F, Zhu W, Gonzalez FJ (2017) Potential role of CYP1B1 in the development and treatment of metabolic diseases. Pharmacol Therapeut 178:18–30. <https://doi.org/10.1016/j.pharmthera.2017.03.007>
4. Liu JW, Pham PT, Skripnikova EV, Zheng SL, Lovings LJ, Wang YJ et al (2015) A Ligand-Based Drug Design. Discovery of 4-trifluoromethyl-7,8-pyrano coumarin as a selective inhibitor of human cytochrome P4501A2. J Med Chem 58:6481–6493. <https://doi.org/10.1021/acs.jmedchem.5b00494>
5. Anandakumar A, Balasubramanian M, Muralidharan R (1986) Nagakesara-a comparative pharmacognosy. Anc Sci Life 4:263–268. <https://www.ancientscienceoflife.org/text.asp?1986/5/4/263/88759>
6. Chanda S, Rakholiya K, Parekh J (2013) Indian medicinal herb: antimicrobial efficacy of *Mesua ferrea* L. seed extracted in different solvents against infection causing pathogenic strains. J Acute Dis 2(4):277–281. [http://dx.doi.org/10.1016/S2221-6189\(13\)60143-2](http://dx.doi.org/10.1016/S2221-6189(13)60143-2)
7. Verotta L, Lovaglio E, Vidari G, Finzi PV, Neri MG, Raimondi A et al (2004) 4-Alkyl- and 4-phenylcoumarins from *Mesua ferrea* as promising multidrug resistant antibacterials. Phytochemistry 65:2867–2879. <https://doi.org/10.1016/j.phytochem.2004.07.001>
8. Chukaew A, Saithong S, Chusri S, Limsuwan S, Watanapokasin R, Voravuthikunchai SP et al (2019) Cytotoxic xanthenes from the roots of *Mesua ferrea* L. Phytochemistry 157:64–70. <https://doi.org/10.1016/j.phytochem.2018.10.008>
9. Zar Wynn Myint K, Kido T, Kusakari K, Prasad Devkota H, Kawahara T, Watanabe T (2021) Rhusflavanone and mesuaferrone B: tyrosinase and elastase inhibitory biflavonoids extracted from the stamens of *Mesua ferrea* L. Nat Prod Res 35(6):1024–1028. <http://dx.doi.org/10.1080/14786419.2019.1613395>

10. Chakraborty DP, Chatterji D (1969) Structure of mesuagin. A new 4-phenylcoumarin. *J Org Chem* 34(12):3784–3786. <https://doi.org/10.1021/jo01264a009>
11. Chakraborty DP, Das BC (1966) The structure of mesuol. *Tetrahedron Lett* 7(46):5727–5730. [https://doi.org/10.1016/S0040-4039\(01\)84186-1](https://doi.org/10.1016/S0040-4039(01)84186-1)
12. Govindachari TR, Pai BR, Subramaniam PS, Ramdas Rao U, Muthukumaraswamy N (1967) Constituents of *Mesua ferrea* L.—II: Ferruol A, a new 4-alkylcoumarin. *Tetrahedron* 23(10):4161–4165. [https://doi.org/10.1016/S0040-4020\(01\)97929-3](https://doi.org/10.1016/S0040-4020(01)97929-3)
13. Guilet D, Helesbeux JJ, Seraphin D, Sevenet T, Richomme P, Bruneton J (2001) Novel Cytotoxic 4-Phenylfuranocoumarins from *Calophyllum dispar*. *J Nat Prod* 64:563–568. <https://doi.org/10.1021/np000517o>
14. Scio E, Ribeiro A, Alves TMA, Romanha AJ, Shin YG, Cordell GA et al (2003) New Bioactive Coumarins from *Kielmeyera albopunctata*. *J Nat Prod* 66:634–637. <https://doi.org/10.1021/np020597r>
15. Reutrakul V, Leewanich P, Tuchinda P, Pohmakotr M, Jaipetch T, Sophasan S et al (2003) Cytotoxic coumarins from *Mammea harmandii*. *Planta med* 69(11):1048–1051. <https://doi.org/10.1055/s-2003-45154>
16. Reyes CR, Estrada ME, Ramirez AT, Amekraz B, Aumelas A, Jankowski CK et al (2004) Cytotoxic effects of mammea type coumarins from *Calophyllum brasiliense*. *Life Sci* 75(13):1635–1647. <https://doi.org/10.1016/j.lfs.2004.03.017>
17. Guilet D, Seraphin D, Rondeau D, Richomme P, Bruneton J (2001) Cytotoxic coumarins from *Calophyllum dispar*. *Phytochemistry* 58(4):571–575. [https://doi.org/10.1016/S0031-9422\(01\)00285-0](https://doi.org/10.1016/S0031-9422(01)00285-0)
18. Go R, Hwang K, Choi K (2015) Cytochrome P450 1 family and cancers. *J Steroid Biochem Mol Biol* 147:24–30. <https://doi.org/10.1016/j.jsbmb.2014.11.003>
19. Yan J, Tung H, Li S, Niu Y, Garbacz WG, Lu P et al (2019) Aryl hydrocarbon receptor signaling prevents activation of hepatic stellate cells and liver fibrogenesis in mice. *Gastroenterology* 157(3):793–806. <https://doi.org/10.1053/j.gastro.2019.05.066>
20. Wang Y, Yang X, Zhu X, Xiao X, Yang X, Qin H et al (2019) Role of Metabolic Activation in Elemicin-Induced Cellular Toxicity[J]. *J Agric Food Chem* 67(29):8243–8252. <https://doi.org/10.1021/acs.jafc.9b02137>

Figures

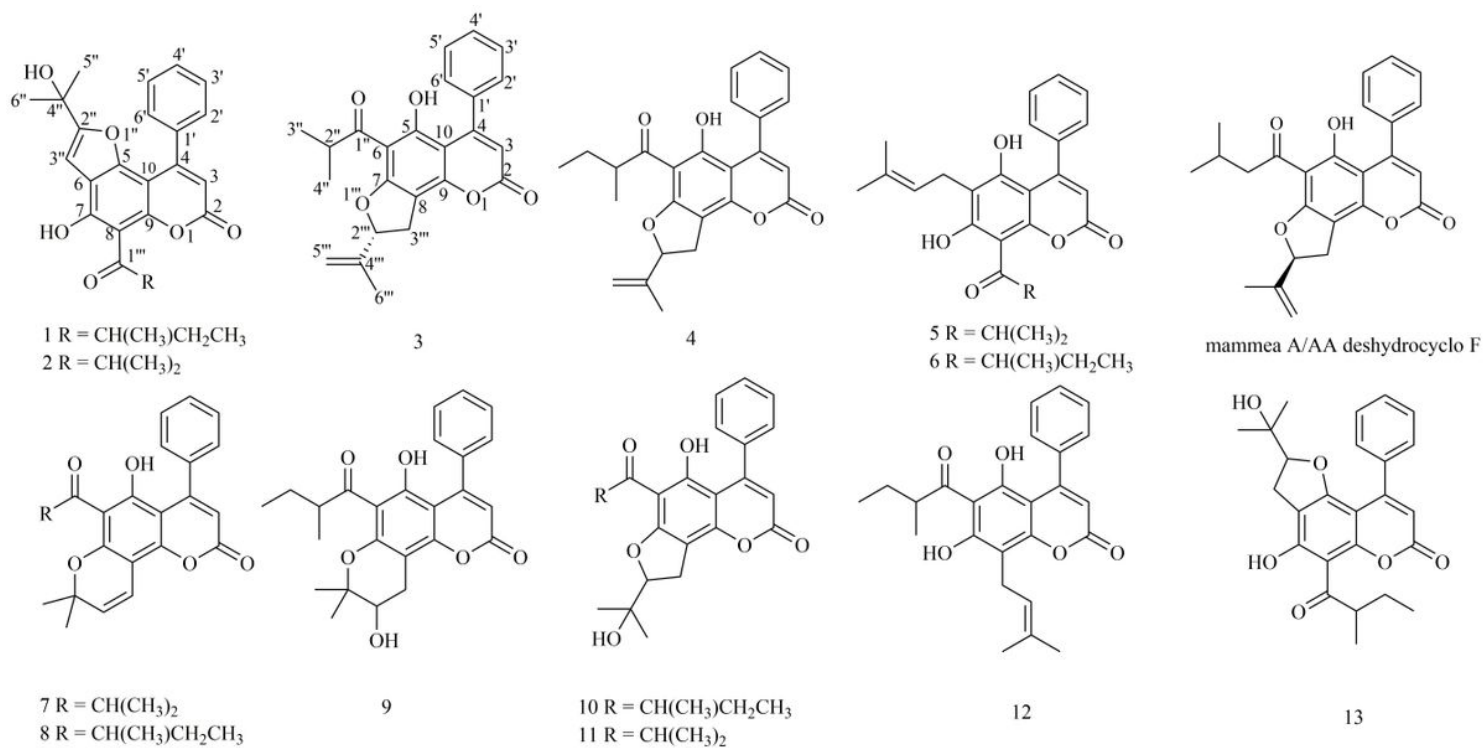


Figure 1

Structures of compounds **1–13** from *Mesua ferrea* Linn.

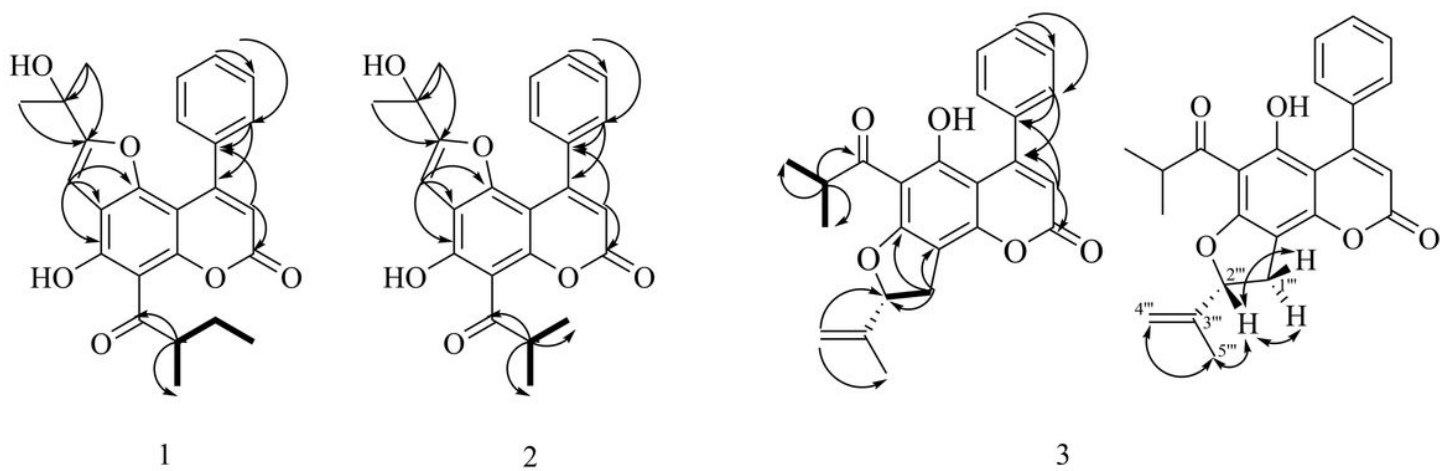


Fig 2 Key ¹H-¹H COSY (—), HMBC (H→C) and ROESY (H↔H) correlations of compounds 1-3

Figure 2

See image above for figure legend.

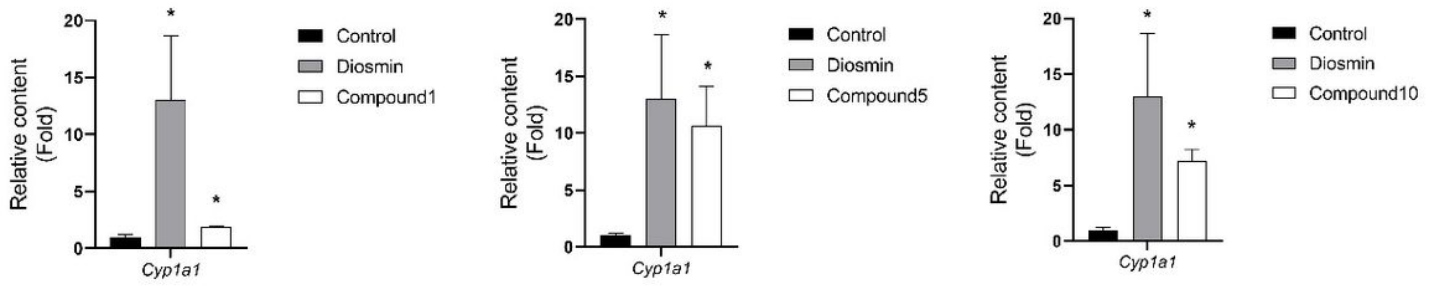


Figure 3

QPCR result about the expression of CYP1A1 (n=4)

*P<0.05, compared with the control group, there is significant difference as indicated

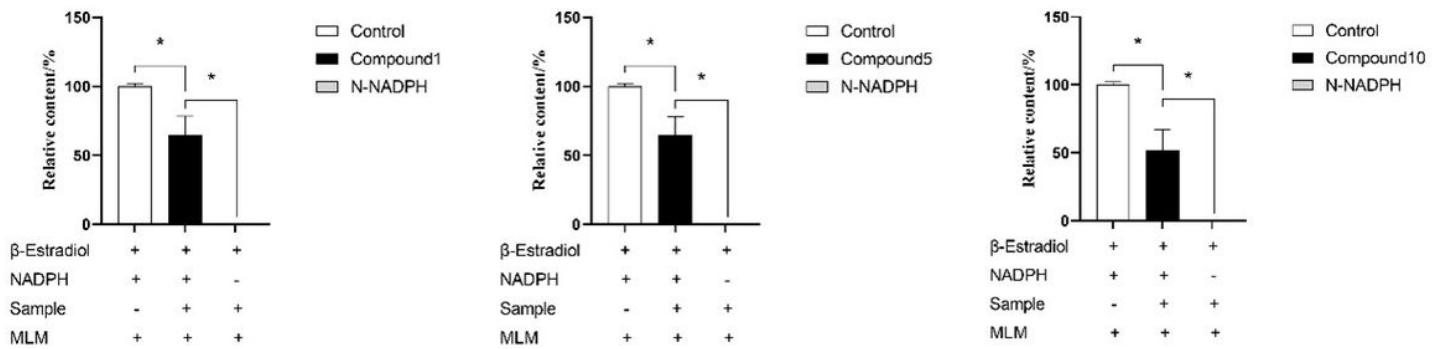


Figure 4

Inhibitory activities of CYP1B1 with NADPH and without NADPH.

*P<0.05, compared with the control group, there is significant difference as indicate

Supplementary Files

This is a list of supplementary files associated with this preprint. Click to download.

- [SupplementaryInformation.docx](#)